

12-29-1994

Reconstructions of C60 on the Ag(111)1x1 Surface

X. -D. Wang
Tohoku University

S. Yamazaki
Tohoku University

J. -L. Li
Tohoku University

T. Hashizume
Tohoku University

H. Shinohara
Nagoya University

See next page for additional authors

Follow this and additional works at: <https://digitalcommons.usu.edu/microscopy>

 Part of the [Biology Commons](#)

Recommended Citation

Wang, X. -D.; Yamazaki, S.; Li, J. -L.; Hashizume, T.; Shinohara, H.; and Sakurai, T. (1994) "Reconstructions of C60 on the Ag(111)1x1 Surface," *Scanning Microscopy*: Vol. 8 : No. 4 , Article 25.

Available at: <https://digitalcommons.usu.edu/microscopy/vol8/iss4/25>

This Article is brought to you for free and open access by the Western Dairy Center at DigitalCommons@USU. It has been accepted for inclusion in Scanning Microscopy by an authorized administrator of DigitalCommons@USU. For more information, please contact digitalcommons@usu.edu.



Reconstructions of C60 on the Ag(111)1x1 Surface

Authors

X. -D. Wang, S. Yamazaki, J. -L. Li, T. Hashizume, H. Shinohara, and T. Sakurai

RECONSTRUCTIONS OF C₆₀ ON THE Ag(111)1x1 SURFACE

X.-D. Wang, S. Yamazaki, J.-L. Li, T. Hashizume, H. Shinohara¹ and T. Sakurai*

The Institute for Materials Research, Tohoku University, Sendai 980, Japan

¹Faculty of Science, Nagoya University, Nagoya 464, Japan

(Received for publication July 7, 1994 and in revised form December 29, 1994)

Abstract

We report the scanning tunneling microscope (STM) study of the C₆₀ adsorption on the Ag(111)1x1 surface. The well-ordered C₆₀ monolayer with good quality was obtained by briefly annealing the multilayer C₆₀ at approximately 300°C. It is concluded that the (2√3)x(2√3)R30° reconstruction is energetically the most stable phase, while two other phases, "hex-a" and "hex-b" phases, are also observed, rotated by approximately 12.5 ± 1.5° and 47.5 ± 1.5° with respect to the stable (2√3)x(2√3)R30° phase. It is suggested that some specific stable adsorption sites are responsible for the pinning and growth of these "hex-a" and "hex-b" phases. Orientational ordering is also documented based on the observed high resolution structures.

Key Words: Scanning tunneling microscope, C₆₀, Ag(111), reconstruction.

Introduction

The interest in the fullerene-metal interaction has been increasing rapidly since the breakthrough in producing fullerenes in macroscopic amounts (Krätschmer *et al.*, 1990). Scanning tunneling microscopy (STM) has proven to be very powerful in studying adsorption and film growth of fullerenes on various surfaces (see, for example, Li *et al.*, 1991a, 1991b; Wilson *et al.*, 1990; Wragg *et al.*, 1990; Zhang *et al.*, 1992) as well as the characterization of the intramolecular structures of fullerenes. The STM studies of C₆₀ adsorbed on the noble metal surfaces, such as Cu (Hashizume *et al.*, 1993; Motai *et al.*, 1993), Ag (Altman and Colton, 1993a, 1993b), and Au (Altman and Colton, 1992; Chen *et al.*, 1992; Howells *et al.*, 1992; Kuk *et al.*, 1993; Wilson *et al.*, 1990; Wragg *et al.*, 1990; Zhang *et al.*, 1992) surfaces, have been reported. On the Cu(111) surface, it is found that the well ordered 4x4 reconstruction can be formed after a brief annealing at ~290°C and that the intramolecular structures are also observed. This is the first case where it was clearly demonstrated that the Cu(111) surface ratchets the rotation of C₆₀ molecules and that the orientational ordering takes place. Photoemission studies concluded that a significant amount of charge transfers to the first layer of C₆₀ from Cu, as well as Au and Ag substrates (Chase *et al.*, 1992; Maxwell *et al.*, 1994; Rowe *et al.*, 1992), similar to the case of alkali metal doping in the C₆₀ bulk phase.

The Ag(111) surface is also found to be a suitable substrate for the film growth of C₆₀, since the (2√3)x(2√3)R30° structure is found to have almost the same lattice constant (10.02 Å) as that of the C₆₀ face centered cubic (fcc) crystal. The adsorption of C₆₀ on Ag(111) was first studied by Altman and Colton (1993a, 1993b). Their results show that the (2√3)x(2√3)R30° reconstruction is the dominant phase on the as-deposited surface at room temperature, while two other phases, rotated 10° and 15° from the <110> direction of the Ag(111) surface, respectively, were also observed in some small areas and it was speculated that they form as the result of growth from the <112̄>, <113̄> or

*Address for correspondence:

Toshio Sakurai
The Institute for Materials Research,
Tohoku University,
Sendai 980,
Japan

Telephone number: 81-22-215-2021

FAX number: 81-22-215 2020

$\langle 11\bar{4} \rangle$ step edges. They also discussed the adsorption geometry of C_{60} molecules in the $(2\sqrt{3}) \times (2\sqrt{3}) R30^\circ$ phase. However, little was discussed about the structure of their reconstructions and stability. The detailed description of these reconstructions, as well as the adsorption geometry of C_{60} molecules in these reconstructions, are still not available.

In this paper, we report the STM study of the C_{60} molecules adsorbed on the Ag(111)1x1 surface. We emphasize here the behavior of the first layer of C_{60} in order to characterize the reconstructions of C_{60} with the Ag substrate. Our results show that even though the $(2\sqrt{3}) \times (2\sqrt{3}) R30^\circ$ phase is the dominant phase on the Ag(111) surface, other phases are also found to be stable at room temperature, with almost the same nearest neighbor (n.n.) distance as that for both the C_{60} fcc bulk phase (10 Å) and the $(2\sqrt{3}) \times (2\sqrt{3}) R30^\circ$ phase. The stability of these phases is studied by annealing the surface at moderate temperatures. The observed intramolecular structures show that the orientational ordering is rather complicated compared to the case of C_{60} on the Cu(111) surface (Hashizume *et al.*, 1993; Motai *et al.*, 1993).

Experiment

The STM instrumentation has been reported elsewhere in detail (see Hashizume *et al.*, 1991; Sakurai *et al.*, 1990). Briefly speaking, our FI-STM is a combination of a high performance scanning tunneling microscope (STM) and a room temperature field ion microscope (FIM) which is used for precise characterization of the scanning tip and its atomic scale fabrication. To obtain excellent stability and duty-cycle performance, $\langle 111 \rangle$ oriented single crystal tungsten tips are used. The single Ag(111) crystal surfaces are cleaned by several cycles of 500 eV Ar^+ bombardments and post-annealings at approximately 420°C until the clean 1x1 surface is obtained by the STM and low energy electron diffraction (LEED).

Briefly speaking, to obtain fullerenes, an arc between two graphite rods was sparked at 200-250 A in the direct current (dc) mode in a He (100-200 Torr) atmosphere to produce fullerene rich soot. The soot was first rinsed with boiling benzene. The solution was refluxed with quinoline, filtered and then concentrated. The condensed powder was rinsed with hexane, methanol, and benzene. The isolation of C_{60} was achieved by the two-stage high-performance liquid chromatography (HPLC). The purity was tested by laser-desorption time-of-flight (LD-TOF) mass spectrometry measurements. It is estimated to be better than 99.5% by LD-TOF mass spectrometry measurements (for more details, see: Saito *et al.*, 1991; Shinohara *et al.*, 1992). The C_{60} powder is placed inside a small Ta-made dispenser

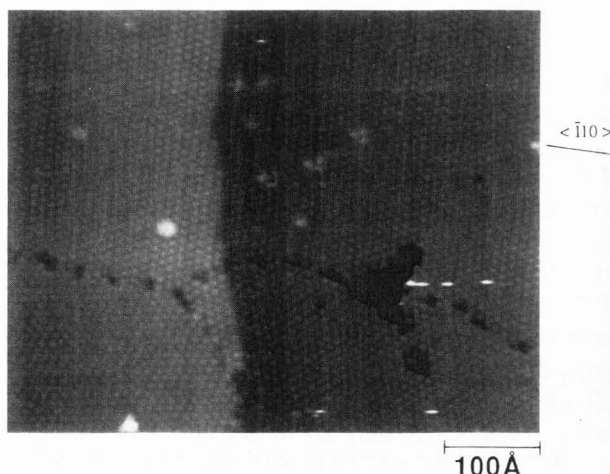


Figure 1. The as-deposited first layer C_{60} on the Ag(111) surface. The domain at the upper part of the image is the $(2\sqrt{3}) \times (2\sqrt{3}) R30^\circ$ phase, the domain at the lower-left part is rotated 12° from the $\langle \bar{1}10 \rangle$ direction, and the domain lower-right part is rotated 46° from the $\langle \bar{1}10 \rangle$ direction. Note that the C_{60} molecules in the $(2\sqrt{3}) \times (2\sqrt{3}) R30^\circ$ phase are imaged with uniform brightness. Sample bias $V_b = -2.0$ V; tunneling current $I_t = 30$ pA.

(Hashizume *et al.*, 1992). After degassing the dispenser thoroughly in a ultra-high vacuum (UHV) preparation chamber, it is brought near the clean sample surfaces and heated at approximately 310°C for sublimation. In all cases, the Ag surface was kept at room temperature during deposition and STM measurements.

Results

The behavior of the initial stage adsorption of C_{60} on Ag(111) is very similar to the case of C_{60} on the Cu(111) surface (Motai *et al.*, 1993). The C_{60} molecules are very mobile on the Ag(111) terrace even at room temperature and they prefer to adsorb and nucleate at the step edges, where the monolayer C_{60} islands start to grow to the terraces. This is also consistent with the STM observation reported by Altman and Colton (1993a, 1993b). The close-packed hexagonal arrangement of C_{60} molecules are observed for the first layer as well as the multiple layers. Careful examination of the STM images shows that in most areas, C_{60} molecules form the hexagonal packing $(2\sqrt{3}) \times (2\sqrt{3}) R30^\circ$ reconstruction, which has the n.n. distance of 10.0 Å. However, several other reconstructions also exhibiting close-packed hexagonal arrays can be frequently observed; the n.n. distances in all these phases are measured to be 10.0 ± 0.1 Å, the same as in the $(2\sqrt{3}) \times (2\sqrt{3}) R30^\circ$ phase. Figure 1 shows the surface of the as-deposited

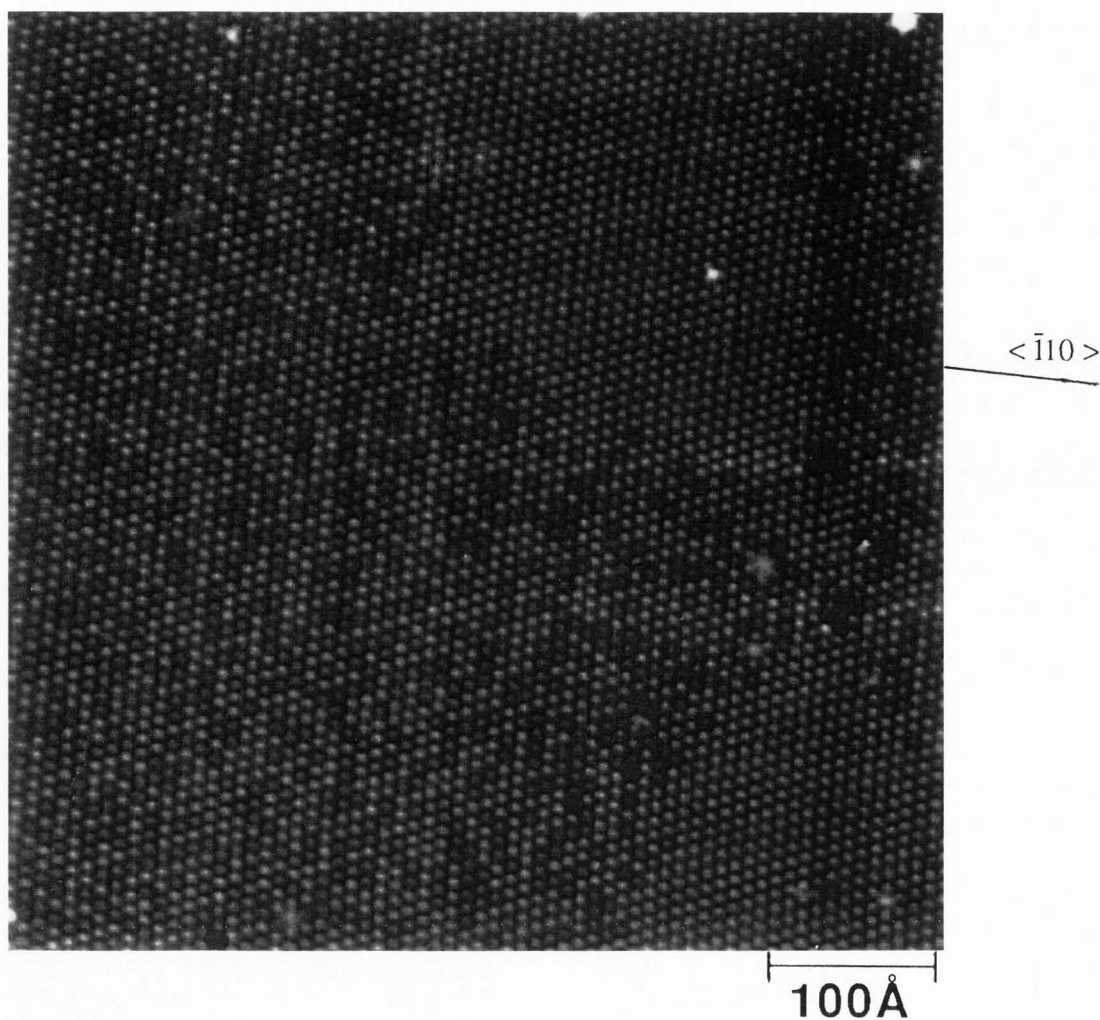


Figure 2. The STM image of a large domain of the $(2\sqrt{3}) \times (2\sqrt{3})R30^\circ$ phase, which is obtained after a brief annealing of the surface at approximately 300°C . It can be observed that the large area is characterized with mixing of dim and bright C_{60} molecules, while the aggregation of bright C_{60} can be seen in the right part of the image.

monolayer C_{60} which contains three different phases. The upper portion of the image is the region of $(2\sqrt{3}) \times (2\sqrt{3})R30^\circ$; the domain in the lower-left part is the same close-packing but is rotated 12° from the $\langle \bar{1}10 \rangle$ direction, while the domain in the lower-right part is rotated 46° from the $\langle \bar{1}10 \rangle$ direction. Similarly, we have observed other phases, which are rotated with certain angles with respect to the $\langle \bar{1}10 \rangle$ direction. In most cases, these angles can be grouped into two types: one has angles between approximately $11\text{--}14^\circ$, which is named as the "hex-a" phase here, and the other one has angles of approximately $46\text{--}49^\circ$ with respect to the $\langle \bar{1}10 \rangle$ direction and is named as "hex-b" phase here. It should be noted that in the as-deposited $(2\sqrt{3}) \times (2\sqrt{3})R30^\circ$ phase, as well as in all other phases, all individual C_{60} adsorbates are imaged with almost equal brightness.

It is found that these reconstructions change upon annealing the surface at moderate temperatures. A brief annealing of the surface of multilayer adsorbed C_{60} film at 300°C results in the C_{60} monolayer on the Ag surface, similar to the case of C_{60} on the Cu(111) surface (Hashizume *et al.*, 1993; Motai *et al.*, 1993). Essentially the same results were obtained by annealing the surface of just one monolayer C_{60} film. For the phases other than the $(2\sqrt{3}) \times (2\sqrt{3})R30^\circ$ phase, individual C_{60} molecules are still imaged with equal brightness. However, a drastic change can be observed in the brightness of the C_{60} images in the $(2\sqrt{3}) \times (2\sqrt{3})R30^\circ$ phase, i.e., C_{60} molecules are imaged with two different kinds of brightness, namely dim C_{60} s and bright C_{60} s. Figure 2 is the STM image of a large terrace of the $(2\sqrt{3}) \times (2\sqrt{3})R30^\circ$ phase after annealing at 300°C briefly. The distribution of the dim and bright C_{60} s can be

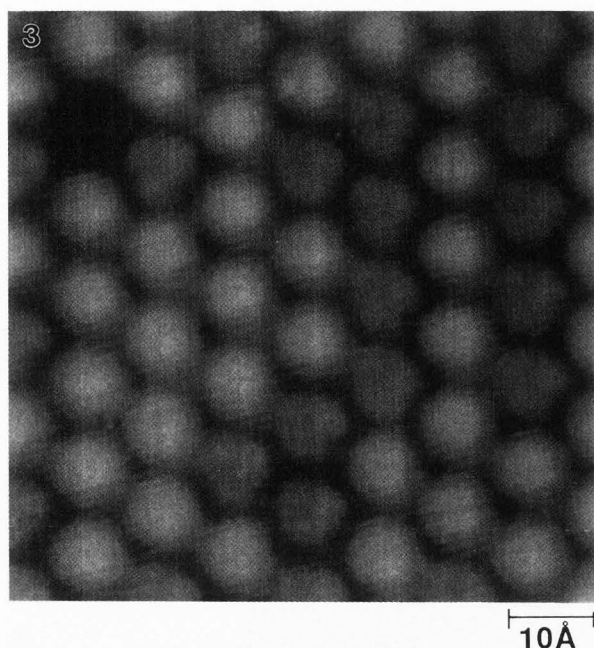


Figure 3. The STM image showing the intramolecular structures of C_{60} in the $(2\sqrt{3})\times(2\sqrt{3})R30^\circ$ phase. (It = 30 pA, $V_b = -1.2$ V).

clearly observed. The apparent height difference between these two kinds of molecules is as large as 0.6 Å at -1.2 V sample bias voltage. It is interesting to note that, although most of the area is characterized with the random mixing of dim and bright C_{60} molecules, the aggregation of bright C_{60} molecules can also be observed in some patches, as shown in the central-upper part of Figure 2. In the area where bright and dim C_{60} molecules are mixed, the portion of the dim C_{60} molecules is approximately 38%. This value does not change even upon prolonged annealing up to 36 hours. Since the fullerene powder is of high purity, it is ruled out that the observed brightness variation is due to the presence of other larger fullerenes, such as C_{70} or C_{84} . We also note that the prolonged annealing up to 36 hours also results in the disappearance of the "hex-a" phase and the "hex-b," leaving only the $(2\sqrt{3})\times(2\sqrt{3})R30^\circ$ phase on the entire surface. This fact suggests that the $(2\sqrt{3})\times(2\sqrt{3})R30^\circ$ phase is energetically the most stable.

The intramolecular structures for the three phases have been observed on the surface after a brief annealing at $\sim 300^\circ\text{C}$. Figure 3 shows the high resolution STM image of the monolayer C_{60} in the $(2\sqrt{3})\times(2\sqrt{3})R30^\circ$ phase at -1.2 V sample bias voltage. In this image, the intramolecular structures of C_{60} molecules can be observed. The intramolecular structures for the dim C_{60} molecules show a three-fold clover-like shape, with their leaves aligning to the close-packed chains of C_{60} molecules. Only faint contrast variations are observed for

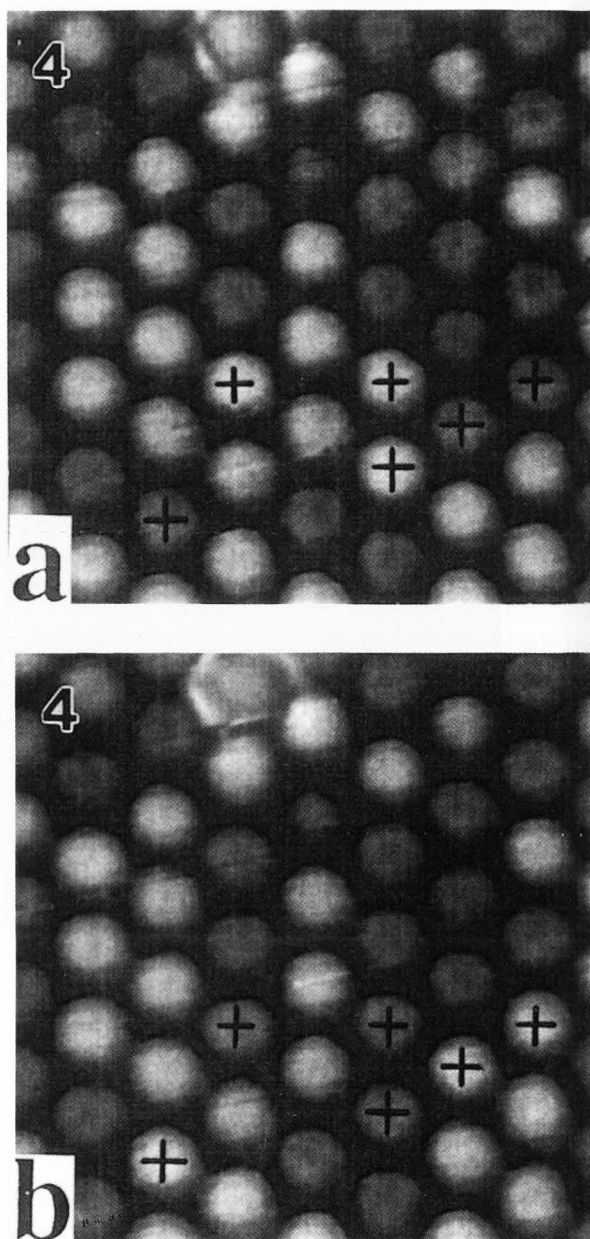


Figure 4. The orientation change as the function of time: (a) The STM image of the surface area with $(2\sqrt{3})\times(2\sqrt{3})R30^\circ$ reconstruction, and (b) the same surface area scanned after 3 minutes later. Note the molecules marked have switched from dim to bright or vice versa.

bright C_{60} molecules. Three-fold images can be observed for dim C_{60} molecules in a wide voltage range of +2.5 V to -2.5 V sample bias voltages, even though the contrast and brightness vary. It is interesting to note that, by continuously scanning the same area at the same scanning conditions, some C_{60} adsorbates change bright-

ness, from "dark" to "bright" and vice versa, as shown in Figures 4a and 4b, obtained in a 3 minute interval.

Figures 5a and 5b show the intramolecular structures of C₆₀s in the "hex-a" phase and "hex-b" phase, respectively, which were also obtained after a brief annealing of the surface at approximately 300°C. Again, the three-fold clover-like features can be well resolved for most C₆₀ molecules. However, these clover-like features are not as symmetric as those observed for the $(2\sqrt{3}) \times (2\sqrt{3}) R30^\circ$ phase. Furthermore, their orientations vary and are irregular. In contrast to the case for the $(2\sqrt{3}) \times (2\sqrt{3}) R30^\circ$ phase, their contrast and shape do not change with time.

The STM images for all the phases of the first layer can be stably observed at sample bias voltages as low as ± 0.1 V, implying their metallic nature.

Discussion

The coexistence of several domains with the same close-packing but different orientation indicates that the difference in adsorption energy for different phases is small. The orientation of a particular domain may simply be determined by the initial nucleation conditions. As the nucleation starts from the step edge, the structure of the step edge may influence the domain orientation. Altman and Colton (1993b) suggested that the alignment of C₆₀ molecules at the step edge at the initial stage adsorption determine the orientation of the domain. The R10° and R15° rotated domains, which they observed, were explained as the growth of C₆₀ molecules at step edges, such as $\langle 11\bar{2} \rangle$, $\langle 11\bar{3} \rangle$ or $\langle 11\bar{4} \rangle$ directions.

However, this interpretation is still not sufficient to explain why only a small number of domains are observed while the orientation of the step edges can be many, depending on the tilting angle of the Ag crystal sample surface off the (111) orientation. Furthermore, even though the $\langle \bar{1}10 \rangle$ step edge is the most stable in energy along with the other two equivalent step edges, $\langle 0\bar{1}1 \rangle$ and $\langle 10\bar{1} \rangle$, we did not observe the phase with its close-packed row parallel to the $\langle \bar{1}10 \rangle$ direction of the substrate step edge. For step edges with the $\langle 11\bar{3} \rangle$ or $\langle 11\bar{4} \rangle$ directions, the close-packed row would have the angle of 13.9°, or of 19.1° with the $\langle \bar{1}10 \rangle$ direction. However, the domain rotated by 19.1° was not documented according to our STM observation. Therefore, other interactions, especially those involving the interactions of C₆₀ with the substrate, must be considered in order to explain the stabilization of the "hex-a" and the "hex-b" phases, as well as the $(2\sqrt{3}) \times (2\sqrt{3}) R30^\circ$; we suggest a specific adsorption geometry with respect to the substrate, as explained below.

Figure 6 shows the models we proposed for the

"hex-a" and the "hex-b" phases. It is assumed in these models that C₆₀s adsorbed at the three-fold hollow sites are the most stable. Even though the actual stable adsorption sites are not known from the present STM observation (for example, it is possible that C₆₀ molecules take the top sites), such an assumption does not adversely affect our conclusion since the assumed three-fold hollow site plays the same role as the real adsorption sites. It can be seen in Figure 6 that the C₆₀ molecules are adsorbed periodically at the three-fold sites if the close-packed arrangement of the C₆₀ layer takes certain specific orientations with angles within $12.5 \pm 1.5^\circ$ with respect to the $\langle \bar{1}10 \rangle$ direction, such arrangements resemble the "hex-a" phase. The shaded molecules serve as the boundary of the unit cells. It is straightforward to understand that for each orientation in Figure 6, equivalent mirror configurations along the $\langle 11\bar{2} \rangle$ axis can be obtained. These reconstructions, with the close-packed row oriented with angles of $47.5 \pm 1.5^\circ$ with respect to the $\langle \bar{1}10 \rangle$ direction form the "hex-b" phase. In all these models, the n.n. distance is less than 1% different from the nominal 10.0 Å, which is within the accuracy of the measured values based on our STM observation.

The observed intramolecular structures of C₆₀ molecules reflect the local charge distribution of electrons within the energy width between the Fermi level and the potential corresponding to the sample bias voltage (Hashizume *et al.*, 1993; Kawazoe *et al.*, 1993; Wang *et al.*, 1993). Therefore, precise interpretation of the intramolecular structures in real space requires the simulation of the band structures theoretically, which is not available presently. However, the observed intramolecular structures still provide the information on the orientation ordering due to the high spatial symmetry of C₆₀ molecules and the substrate. As shown in Figure 3, which is obtained after annealing, in the $(2\sqrt{3}) \times (2\sqrt{3}) R30^\circ$ phase, for the dim C₆₀ molecules, the three-fold features are imaged with almost equal brightness. This indicates that the dim C₆₀ molecules are adsorbed at equivalent positions having the same orientation. In the "hex-a" and "hex-b" phases, however, even though most molecules are imaged with clover-like shape, the orientations of such clover-like shape images vary even in the same domain; and the relative intensities of the three leaves are usually not equal to one another. Such features indicate that the orientation of C₆₀ molecules is not well-ordered. This is likely due to the non-equivalent adsorption sites, i.e., the variation in the bonding configurations for C₆₀ with the Ag(111) substrate, as illustrated in Figure 6. This is also the reason why the "hex-a" and "hex-b" phases are not energetically the most favorable and why they transfer to the $(2\sqrt{3}) \times (2\sqrt{3}) R30^\circ$ phase upon annealing.

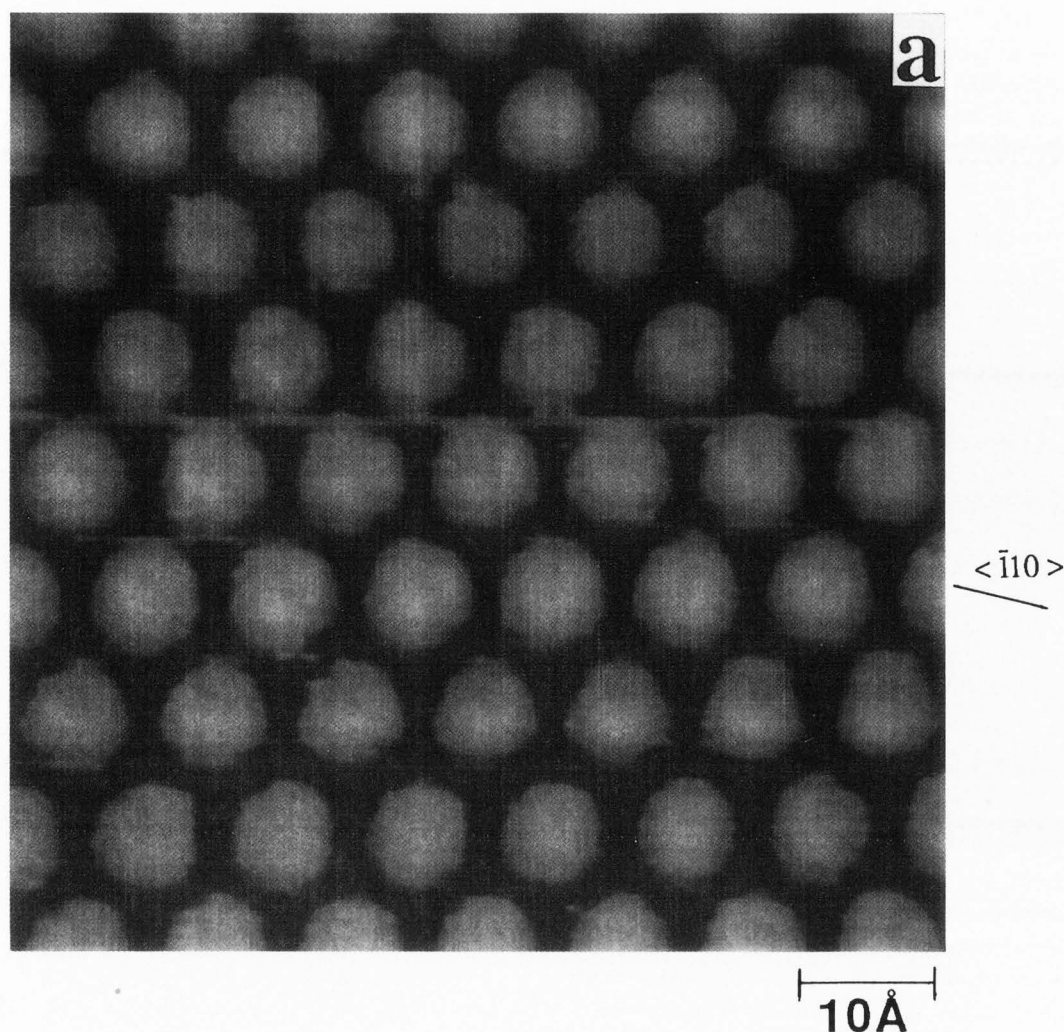
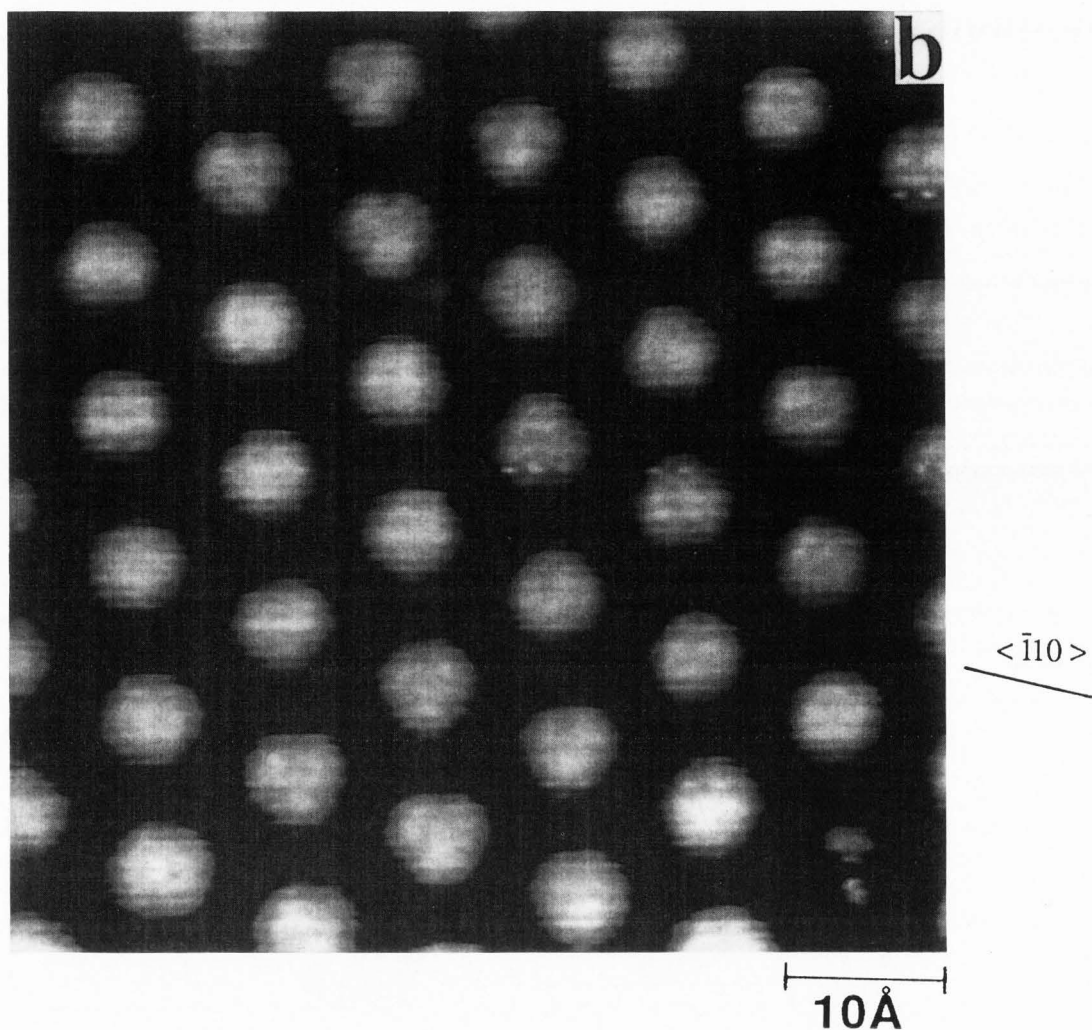


Figure 5. The STM images showing the intramolecular structure of C_{60} in (a, above) the "hex-a" phase ($V_b = -0.5$ V, $I_t = 30$ pA), and (b, on the facing page) "hex-b" phases ($V_b = +0.1$ V, $I_t = 30$ pA).

In the case of the $(2\sqrt{3}) \times (2\sqrt{3}) R30^\circ$ phase, each C_{60} molecule is supposed to reside at the equivalent position, and thus, they should be identical in the STM image. However, the C_{60} molecules are imaged in two kinds of distinct brightness upon a brief annealing, contradicting our assumption sharply. We suggest that such image characteristics are the result of the relaxation of the stress exerted in the C_{60} layer induced by a significant adsorbate-substrate interaction. Although the n.n. distance of C_{60} in the $(2\sqrt{3}) \times (2\sqrt{3}) R30^\circ$ phase is almost exactly the same as the n.n. distance for the fcc bulk crystal, the charge transfer from the Ag substrate, as evident by the STM (Altman and Colton, 1993b) and photoemission studies (Chase *et al.*, 1992; Ohno *et al.*, 1991; Rowe *et al.*, 1992), is likely to induce a repulsive interaction in the C_{60} layer. Such an interaction might increase the n.n. distance for a monolayer C_{60} with re-

spect to the n.n. distance in non-charged C_{60} bulk phase, as well as the lattice constant for $(2\sqrt{3}) \times (2\sqrt{3}) R30^\circ$ reconstruction due to the change of relative strength between attractive and repulsive molecule-molecule interactions, provided that the interaction with the substrate could be neglected. However, due to the stronger interaction between the Ag(111) substrate and C_{60} layer, it is less favorable for the C_{60} layer to reconstruct in a way other than the $(2\sqrt{3}) \times (2\sqrt{3}) R30^\circ$ reconstruction. Therefore, certain stress must be induced due to the competition between these interactions if all the C_{60} molecules stay in equivalent positions. To reduce the stress, some C_{60} molecules may change the adsorption geometry away from their equivalent positions as the intermolecular interaction is anisotropic (Cheng and Klein, 1993; Gao *et al.*, 1991; Soper *et al.*, 1992; Sprik *et al.*, 1992).

As we noted earlier, the switching between dim C_{60}



and bright C_{60} imaging contrast happens very frequently. We conclude that such a variation in brightness for the C_{60} molecules is related to the orientational variation, which corresponds to the variation of the charge distribution, instead of the real height change for the C_{60} molecules. Stress-induced orientational variation is also frequently observed in the domain boundaries where the change of the n.n. distance happens, as well as at some defect sites.

In the $(2\sqrt{3}) \times (2\sqrt{3}) R30^\circ$ phase, the rather small barrier for different orientations, as evidenced with the frequent change between dim and bright C_{60} molecules, may originate from the higher order of symmetry and fitting to the three-fold substrate. In contrast, for "hex-a" and "hex-b" phases, even though these phases are not stable energetically, the orientation of each molecule does not change with time, indicating that the barrier between various orientations is rather high. This is likely due to the different and asymmetric adsorption configurations for C_{60} molecules with each other.

Summary

In conclusion, our STM observations show that the $(2\sqrt{3}) \times (2\sqrt{3}) R30^\circ$ phase is dominant for the first layer adsorption of C_{60} at room temperature, however, several other phases are also observed to have almost the identical n.n. distances as that for the $(2\sqrt{3}) \times (2\sqrt{3}) R30^\circ$ phase, but with several domain orientations. Annealing the surface at about 300°C results in the desorption of the C_{60} s above the first layer and the transition of the entire first layer to the $(2\sqrt{3}) \times (2\sqrt{3}) R30^\circ$ reconstruction finally, thus indicating that this phase is energetically the most stable. It is also found that two types of C_{60} molecular images: dim and bright C_{60} imaging contrast, are observed in the $(2\sqrt{3}) \times (2\sqrt{3}) R30^\circ$ phase after annealing. These two types of images are mixed in most areas; in some areas, however, aggregation of the brightly imaged C_{60} s are observed. This indicates that, in order to release the stress in the adsorbed layer, there exist several adsorption configurations for C_{60} in the

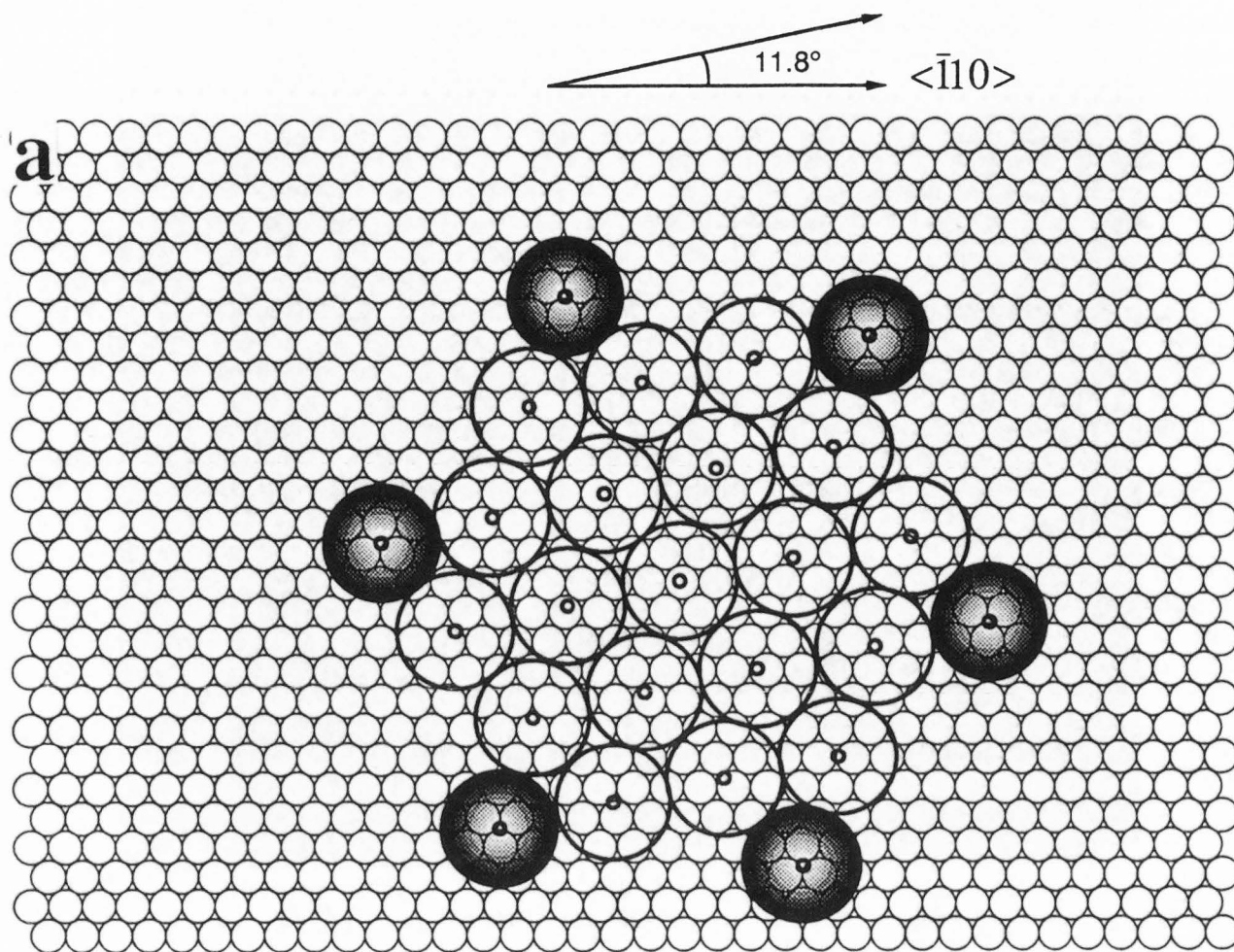
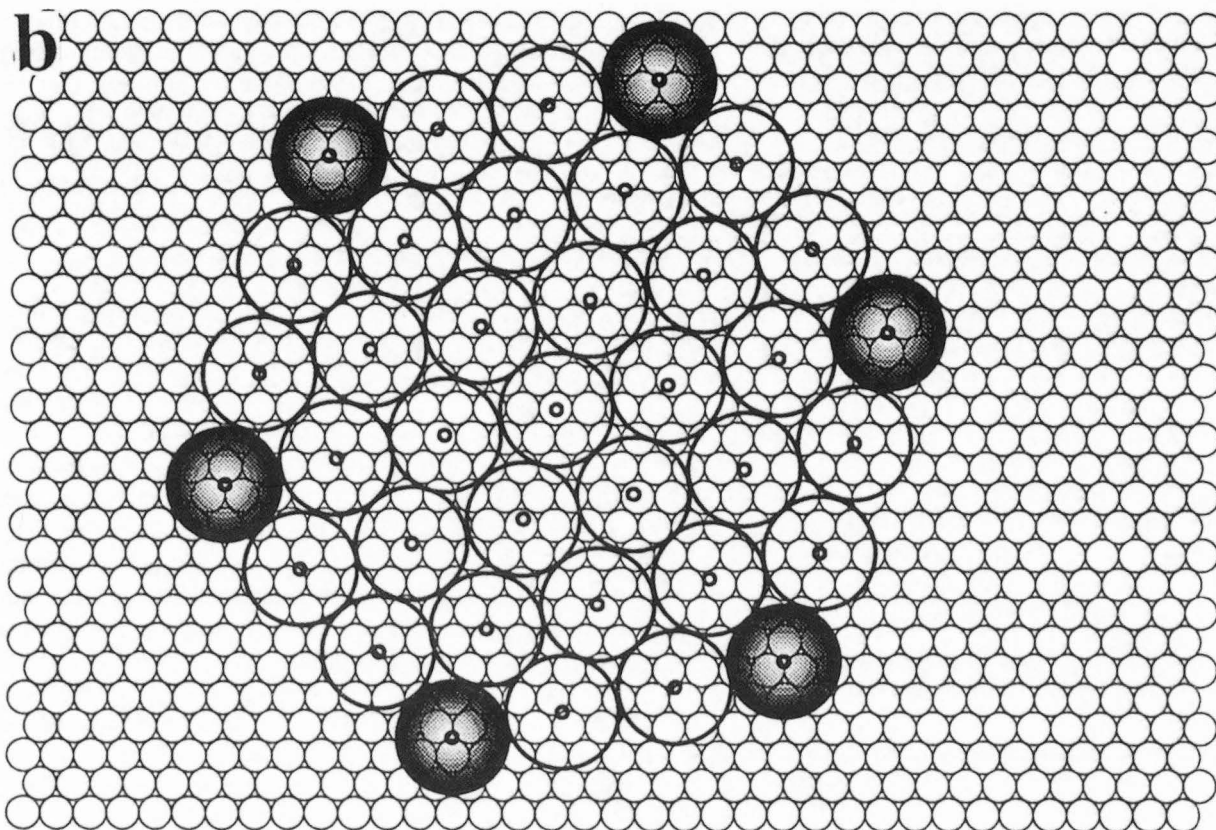
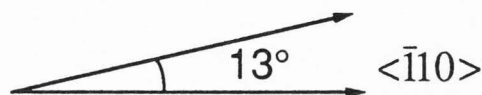
$(2\sqrt{3}) \times (2\sqrt{3}) R11.8^\circ$


Figure 6. Schematic of the reconstructions of the C_{60} first layer on the Ag(111) surface: (a, above) The domain with 11.8° angle rotation with respect to the $\langle \bar{1}10 \rangle$ direction; (b, on the facing page) The domain with 13° angle rotation with respect to the $\langle \bar{1}10 \rangle$ direction. The equivalent mirror configurations of these reconstructions along the $\langle 11\bar{2} \rangle$ axis form the "hex-b" phase, with angles 48.2° and 47° , respectively.

$(2\sqrt{3}) \times (2\sqrt{3}) R30^\circ$ phase even though the $(2\sqrt{3}) \times (2\sqrt{3}) R30^\circ$ reconstruction is completely commensurate with the Ag(111) 1×1 substrate. The intramolecular structures are also observed for all the phases, reflecting the variation of the adsorption geometry and the orientation of the C_{60} molecules.

References

- Altman EI, Colton RJ (1992) Nucleation, growth, and structure of fullerene films on Au(111). *Surf Sci* **279**: 49-67.
- Altman EI, Colton RJ (1993a) The interaction of C_{60} with noble metal surfaces. *Surf Sci* **295**: 13-20.
- Altman EI, Colton RJ (1993b) Determination of the orientation of C_{60} adsorbed on Au(111) and Ag(111). *Phys Rev* **B48**: 18244-18249.
- Chase SJ, Bacsa WS, Mitch MG, Pilione LJ, Lannin JS (1992) Surface-enhanced Raman scattering and photoemission of C_{60} on noble-metal surfaces. *Phys Rev* **B46**: 7873-7877.
- Chen T, Howells S, Gallagher M, Yi L, Sarid D, Lichtenberger DL, Nebesny KW, Ray CD (1992) Internal structure and two-dimensional order of monolayer C_{60} molecules on gold substrate. *J Vac Sci Technol* **B10**: 170-174.
- Cheng A, Klein ML (1993) Solid C_{70} : A molecular-dynamics study of the structure and orientational

$"(2\sqrt{3}) \times (2\sqrt{3})"R13^\circ$ 

ordering. *Phys Rev* **B46**: 4958-4962.

Gao Y, Karasawa N, Goddard III WA (1991) Prediction of fullerene packing in C_{60} and C_{70} crystals. *Nature* **351**: 464-467.

Hashizume T, Sumita I, Murata Y, Hyodo S, Sakurai T (1991) Cs adsorption on the Si(100)2x1 surfaces. *J Vac Sci Technol* **A9**: 742-744.

Hashizume T, Wang X-D, Nishina Y, Shinohara H, Saito Y, Kuk Y, Sakurai T (1992) Field ion-scanning tunneling microscopy study of C_{60} on the Si(100) surface. *Jpn J Appl Phys* **31**: L880-L883.

Hashizume T, Motai K, Wang X-D, Shinohara H, Saito Y, Maruyama Y, Ohno K, Kawazoe Y, Nishina Y, Pickering H. W, Kuk Y, Sakurai T (1993) Intramolecular structures of C_{60} molecules adsorbed on the Cu(111)-1x1 surface. *Phys Rev Lett* **71**: 2959-2963.

Howells S, Chen T, Gallagher M, Sarid D, Lichtenberger DL, Wright LL, Ray CD, Huffman DR, Lamb LD (1992) High resolution images of single C_{60}

molecules on gold (111) using scanning tunneling microscopy. *Surf Sci* **274**: 141-146.

Kawazoe Y, Kamiyama H, Maruyama Y, Ohno K (1993) Electronic structures of layered C_{60} and C_{70} on Si(100) surface. *Jpn J Appl Phys* **32**: 1433-1437.

Krätschmer W, Lamb LD, Fostiropoulos K, Huffman DR (1990) Solid C_{60} : a new form of carbon. *Nature* **347**: 354-358.

Kuk Y, Kim DK, Suh YD, Park KH, Noh HP, Oh SJ, Kim SK (1993) Stressed C_{60} layers on Au(001). *Phys Rev Lett* **70**: 1948-1951.

Li YZ, Patrin JC, Chander M, Weaver JH, Chibante LPF, Smalley RE, (1991a) Ordered overlayers of C_{60} on GaAs(110) studied with scanning tunneling microscopy. *Science* **252**: 547-551.

Li YZ, Chander M, Patrin JC, Weaver JH, Chibante LPF, Smalley RE (1991b) Order and disorder in C_{60} and K_xC_{60} multilayers: direct imaging with scanning tunneling microscopy. *Science* **253**: 429-433.

Maxwell AJ, Bruhwiler PA, Nilsson A, Mårtensson N, Rudolf P (1994) Photoemission, autoionization, and X-ray-absorption spectroscopy of ultrathin-film C₆₀ on Au(110). *Phys Rev* **B49**: 10717-10725.

Motai K, Hashizume T, Shinohara H, Sakurai T (1993) C₆₀ grown on the Cu(111)1x1 surface. *Jpn J Appl Phys* **32**: L450-L453.

Ohno TR, Chen Y, Harvey SE, Kroll GH, Weaver JH (1991) C₆₀ bonding and energy-level alignment on metal and semiconductor surfaces. *Phys Rev* **B44**: 13747-13755.

Rowe JE, Rudolf P, Tjeng LH, Malic RA, Meigs G, Chen CT, Chen J, Plummer EW (1992) Synchrotron radiation and low energy electron diffraction studies of ultrathin C₆₀ films deposited on Cu(100), Cu(111) and Cu(110). *Int J Mod Phys* **B6**: 3909-3913.

Saito Y, Kurosawa K, Shinohara H, Saito S, Oshiyama A, Ando Y, Noda T (1991) X-ray emission spectrum of solid C₆₀. *J Phys Soc Jpn* **60**: 2518-2521.

Sakurai T, Hashizume T, Kamiya I, Hasegawa Y, Sano N, Pickering HW, Sakai A (1990) Field ion-scanning tunneling microscopy. *Prog Surf Sci* **33**: 3-89.

Shinohara H, Sato H, Saito Y, Izuoka A, Sugawara T, Ito H, Sakurai T, Matsuo T (1992) Extraction and mass spectroscopic characterization of giant fullerenes up to C₅₀₀. *Rapid Commun Mass Spectrom* **6**: 413-416.

Soper AK, David WIF, Sivia DS, Dennis TJS, Hare JP, Prassides KTI (1992) A pair correlation function study of the structure of C₆₀. *J Phys, Condens Matter* **4**: 6087-6094.

Sprink M, Cheng A, Klein ML (1992) Modeling the orientational ordering transition in solid C₆₀. *J Phys Chem* **96**: 2027-2029.

Wang X-D, Hashizume T, Shinohara H, Saito Y, Nishina Y, Sakurai T (1993) Adsorption of C₆₀ and C₈₄ on the Si(100)2x1 surface studied by using the scanning tunneling microscope. *Phys Rev* **B47**: 15923-15930.

Wilson RJ, Meijer G, Bethune DS, Johnson RD, Chambliss DD, de Vries MS, Hunziker HE, Wendt HR (1990) Imaging C₆₀ clusters on a surface using a scanning tunneling microscope. *Nature* **348**: 621-622.

Wragg JL, Chamberlain JE, White HW, Krättschmer W, Huffman DR (1990) Scanning tunneling microscopy of solid C₆₀/C₇₀. *Nature* **348**: 623-624.

Zhang Y, Gao X, Weaver MJ (1992) Scanning tunneling microscopy of C₆₀ and C₇₀ on ordered Au(111) and Au(110): molecular structure and electron transmission. *J Phys Chem* **96**: 510-513.

Discussion with Reviewers

Z.C. Ying: Would the experimental results be the same following heating of a C₆₀ monolayer deposited at room temperature?

Authors: Most of our results were obtained after annealing the multilayer C₆₀ film. However, apparent difference was not observed between annealing multilayer film and monolayer film after a careful examination. The reason we usually anneal multilayer film is that we intend to deposit the amount of C₆₀ slightly more than that estimated for one monolayer to ensure that ALL the surface is covered with C₆₀. A modification is done in the corresponding place of the manuscript to declare this point.

Z.C. Ying: Is the state of mixed orientations the lowest energy configuration, a precursor for monolayer desorption, or a frozen of a high-temperature state? The latter two possibilities could be ruled out if the effects of annealing temperature and cooling rate are known.

Authors: The latter two possibilities can be ruled out according to the observation that the orientation of C₆₀ molecules in the annealed film changes between sequential images recorded, which were obtained in a time scale of a few minutes, while the ratio of bright and dim molecules remained the same during the whole run, which usually lasted for a few days.

Z.C. Ying: Do the C₆₀ molecules, as-deposited on Ag(111) at room temperature, correspond to those in the bright or dim states of the annealed monolayer?

Authors: It is our suspicion that the bright states after annealing correspond to those as-deposited on Ag(111) at room temperature. However, we do not intend to draw any conclusions since, due to the instrumental limitations, we are unable to keep the scanning area, before and after annealing, the same. It is interesting to investigate this issue *in situ* by using high temperature STM in future experiments.

R.J. Colton and E.I. Altman: Do shaded molecules "appear" different on the ratio shaded/unshaded/symmetry (Fig. 6)?

Authors: The shaded molecules in Figure 6 serve as boundaries of the unit cells, not the real adsorption sites. We think that certain adsorption sites, with periodicity shown in Figure 6, as a whole, make those observed reconstructions stable before annealing. However, we do not observe the difference in the STM images for those molecules with different adsorption sites. We believe this is due to the very small difference in adsorption energy and height for those sites, as well as the electronic density of states.